Adaptive optics for in vivo two-photon calcium imaging of neuronal networks

Serge Meimon[a], Jean-Marc Conan[a], Laurent M. Mugnier[a], Vincent Michau[a], Rosa Cossart[b] and Arnaud Malvache[b,c]

[a]Onera - the French Aerospace Lab, F-92322 Châtillon, France;
[b]INMED, INSERM U901, Aix-Marseille Université, BP13 13273 Marseille Cedex 09, France;
[c]Institut Fresnel, UMR 7249 CNRS, Aix-Marseille Université, Domaine Universitaire de St Jérôme 13397 Marseille Cedex 20, France.

ABSTRACT

The landscape of biomedical research in neuroscience has changed dramatically in recent years as a result of spectacular progress in dynamic microscopy. However, the optical accessibility of deep brain structures or deeper regions of the surgically exposed hippocampus (a few 100 microns typically) remains limited, due to volumic aberrations created by the sample inhomogeneities. Adaptive optics can correct for these aberrations. Our goal is to realize a novel adaptive optics module dedicated to *in vivo* two-photon calcium imaging of the hippocampus. The key issue in adaptive optics is the ability to perform an accurate and reliable wavefront sensing. In two-photon microscopy indirect methods are required. Two families of approaches have been proposed so far, the modal sensorless technique and a method based on pupil segmentation. We present here a formal comparison of these approaches, in particular as a function of the amount of aberrations.

Keywords: neurobiology ; microscopy ; adaptive optics.

1. INTRODUCTION

The landscape of biomedical research in neuroscience has changed dramatically in recent years as a result of spectacular progress in dynamic microscopy. Significant developments in imaging (scanning laser microscopy, photomultiplication) and illumination (femtosecond laser pulses) technology have triggered an improvement of the spatio-temporal resolution reached on *in vivo* movies. However, the optical accessibility of deep brain regions (a few 100 microns typically) remains limited, due to volumic aberrations created by the sample inhomogeneities.

The present project is motivated by an existing neurobiology experiment, the description of spatio-temporal patterns of neuronal activation in cortical networks by Dr. Cossart's team at INMED.[1,2] This experiment relies on two-photon calcium imaging using a genetically encoded calcium indicator (GCaMP6, see Chen *et al.* Nature 2013). Since intracellular calcium rises indirectly report neuronal spiking, this non-invasive high resolution technique allows to visualize the activity of hundreds of neurons in awake mice. A mathematical processing of the recorded activity allows to reconstruct functional connexions between neurons, leading to a mapping of the functional organization of the imaged neuronal network. In this kind of experiments, spatial resolution and accessible depth are critical parameters, currently limited by the wavefront distortion due to the optical inhomogeneities of the tissue.

Adaptive optics (AO) is a technology allowing to precompensate the illumination laser, provided that the wavefront (aberrations) is correctly measured. In the context of *in vivo* two photon microscopy, such a wavefront sensing is particularly difficult, and has to be done via an "indirect" measurement based on the observation of the scene itself.[3–5] A promising demonstration of an indirect *in vivo* measurement has already been published[6] but it only constitutes a first step towards an optimal use of AO.

Our final goal is to develop an efficient indirect wavefront sensing approach leading to a tomographic measurement of the aberrations, and to define a correction scheme by adapting the latest developments in wide field

Further author information: Send correspondence to meimon@onera.fr

MEMS Adaptive Optics VIII, edited by Thomas G. Bifano, Joel Kubby, Sylvain Gigan, Proc. of SPIE Vol. 8978, 89780C · © 2014 SPIE · CCC code: 0277-786X/14/$18 · doi: 10.1117/12.2044052

AO for astronomy (see for instance AO4ELT3 proceedings at http://ao4elt3.sciencesconf.org/). The obtained AO assisted two photon scanning microscope will be applied to *in vivo* calcium imaging of the hippocampus, after surgical resection of the overlying cortex, aiming at understanding the functional architecture of neuronal networks involved in spatial coding, memory and epilepsy. Such an imaging experiment, featuring a wide field of view (500× 500 microns), with a high numerical aperture ($NA \approx 1$), will require a wavefront correction that evolves with the field.

The present paper concentrates on a formal comparison of the two current main wavefront sensing approaches: modal sensorless method[3,7,8] and pupil segmentation method.[4,6]

We first recall in Sect. 2 the indirect wavefront strategies. We evaluate the return flux as a function of numerical aperture in Sect. 3. We then present a qualitative analysis of the pros and cons of the two considered approaches in Sect. 4.

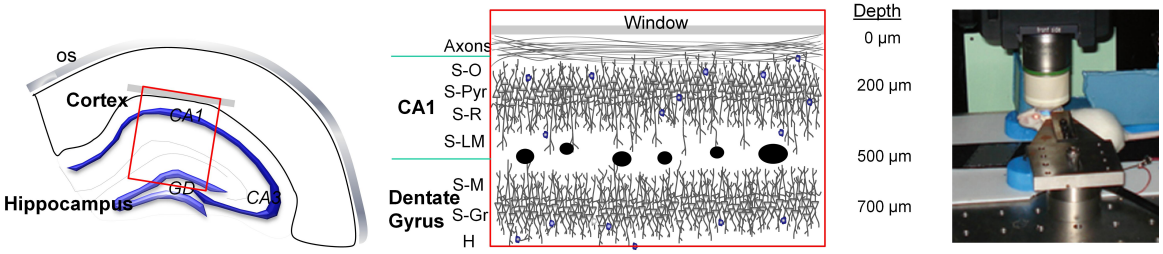

Figure 1. Sketch describing the principle of the experiment: *in vivo* imaging of the mouse hippocampus (CA1 and Dentate Gyrus) by two-photon scanning microscopy: (left) Coronal view of the hippocampus and the overlying cortex (center) Schematics of hippocampal layers (right) Picture of the living mouse head-fixed under the microscope objective.

2. WAVEFRONT SENSING FOR TWO-PHOTON MICROSCOPY

Adaptive optics, widely used in astronomy, has found a particularly promising field of application in two-photon scanning microscopy where scattering effects are not dominant: what remains is essentially phase aberration effects, which is precisely where AO comes into play.[9] Several wavefront sensing approaches in two-photon microscopy have been proposed, using either full pupil imaging with a clever phase modulation,[3] so-called modal sensorless method, or imaging with a pupil segmentation.[4,6]

Modal sensorless wavefront sensing is based on an iterative procedure that aims at optimizing the deformable mirror correction in order to optimize an image quality metric (see illustration on Fig. 2). In two-photon microscopy Débarre *et al.*[3] selected, as a metric, the maximization of the return flux. They have shown that this criterion can be expressed, in the small phase approximation, as a quadratic form in the aberration coefficients. The optimum aberration coefficients can then be deduced from full aperture scan images recorded with an adequate sequence of trial aberrations. For a correction by N aberration modes, one has to record $(P-1).N+1$ or $P.N$ scans, with P between 3 and 9, depending on the chosen trial strategy.[8] This technique has been demonstrated with great success on *ex vivo* biological samples.[7,8] Other phase modulation approaches are also under study and have been tested *ex vivo*.[5]

The pupil segmentation technique is quite different. It is based on the acquisition of sub-pupil scan images, the various sub-pupils being distributed so as to pave the full pupil. Ji *et al.*[4] have shown (see Fig. 3 for illustration) that shifts observed between two sub-pupil scan images are related to the differential wavefront slope (local tilt) between sub-pupils. This approach can therefore be seen as an adaptation of the Shack-Hartmann wavefront sensor to the context of laser scanning two-photon imaging where the return beam can not be directly used for wavefront sensing. A promising *in vivo* demonstration of this technique has recently been published,[6] opening the path to AO developments for deep *in vivo* two-photon scanning microscopy.

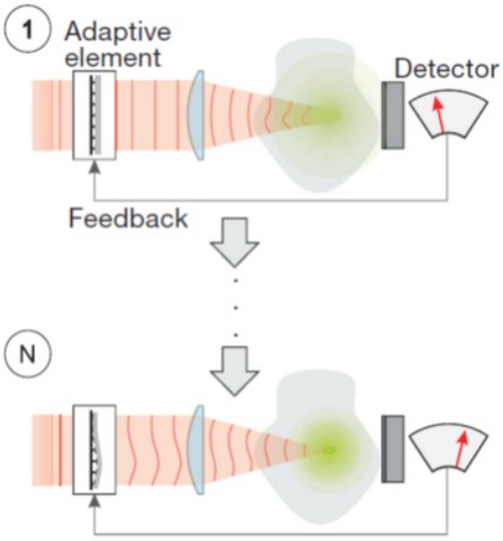

Figure 2. Principle of the modal sensorless method (illustration extracted from[9]).

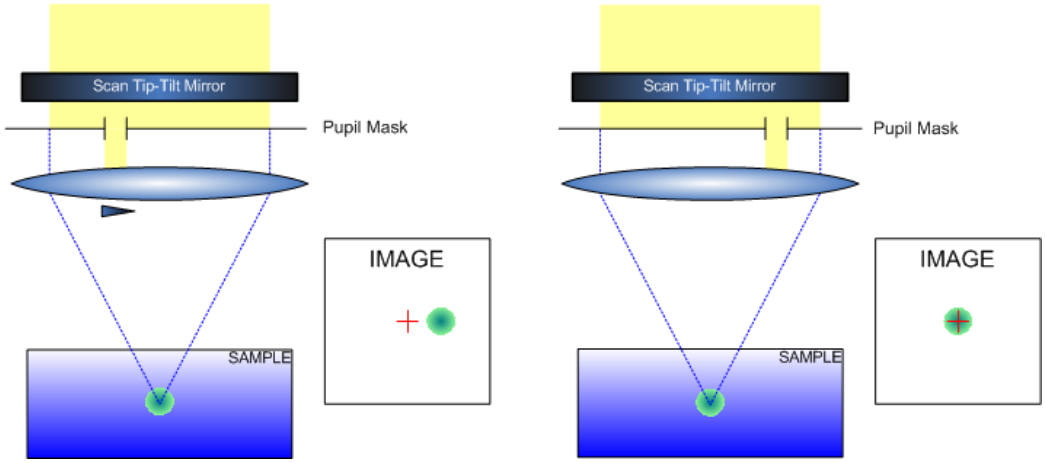

Figure 3. Principle of the pupil segmentation method.[4]

3. RETURN FLUX ASSESSMENT

3.1 Illumination beam

The beam geometry is described in Fig. 4. Let us first assume that the illumination beam is a perfect Gaussian beam focused in the biological tissue with a given numerical aperture NA. The transverse resolution r_{xy} corresponds to the spot size at the best focus, which can be defined as twice its waist, hence $r_{xy} = 2w_0 = \frac{2\lambda}{\pi \mathrm{NA}}$. The longitudinal resolution r_z can be defined as twice the Rayleigh length, hence $r_z = \frac{2\lambda}{\pi \mathrm{NA}^2}$. More generally the beam section in the focal volume is characterized by the waist $w(z)$ given by: $w^2(z) = w_0^2\left(1 + \left(\frac{\lambda z}{\pi w_0^2}\right)^2\right) = w_0^2 + \mathrm{NA}^2 z^2$ where z is the distance to the focal plane.

In a given transverse plane z, the integral of the irradiance (square modulus of the amplitude) is equal to the global laser power P reaching this plane. In the following we make an additional simplification: the Gaussian beam is approximated by a uniform disk of radius $w(z)$. The point spread function in irradiance is then given by $PSF(x, y, z) = \frac{P}{\pi w(z)^2}$ inside the illuminated disk, and 0 elsewhere.

Note that in the presence of optical aberrations the beam radius at best focus w_1 becomes larger than the diffraction limited waist w_0, and one can write : $w_1^2 = w_0^2 + w_{aber}^2$ where w_{aber} is a parameter that characterizes

the resolution loss induced by the aberrations; this term is assumed here to be independent of NA, even if in practice there will be a weak dependence.

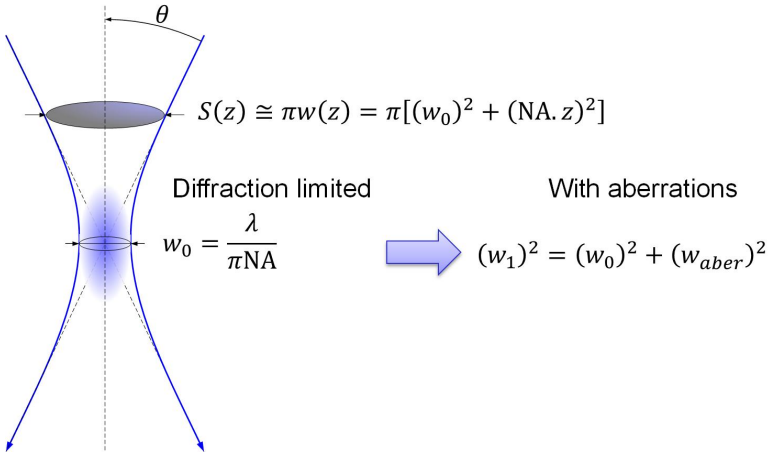

Figure 4. Geometry of the illumination beam.

3.2 Object model

In two-photon microscopy the illumination beam excites fluorophores located in the neuron cytoplasm. A neuron is a roughly spherical cell of about $15\mu m$ in diameter, with a cytoplasm of a few microns thickness.

When diffraction limited and at full aperture (NA $\simeq$ 1) the transverse and longitudinal resolutions are micrometric for a wavelength of about $1\mu m$. When considering smaller apertures, or in the presence of aberrations, the transverse resolution may become a few microns, while longitudinal resolution reaches tens of microns.

Since on the one hand the longitudinal resolution is of the order of, or larger than, the cytoplasm thickness, and on the other hand the transverse resolution is significantly smaller than the neuron size, we approximate the intersection of the Gaussian beam with the neuron cytoplasm by the intersection with a thin 2D plane at the best focus, that is at $z = 0$.

3.3 Return flux trend

In two-photon microscopy the return flux F_r is proportional to the integral of square of the PSF in irradiance weighted by the fluorescence efficiency distribution in the volume. With the hypothesis made in Sect. 3.1 and 3.2, we have:

$$\begin{aligned} F_r &\propto \int\int PSF^2(x, y, z = 0)\mathrm{d}x\mathrm{d}y \\ &\propto \frac{1}{\left(\frac{\lambda}{\pi \mathrm{NA}}\right)^2 + w_{aber}^2} \end{aligned} \tag{1}$$

3.4 Aberration regimes

Figure 5 shows the evolution of the return flux F_r with the Numerical Aperture (or conversely the diameter of the aperture) for a given aberration resolution loss w_{aber}. A saturation due to the w_{aber} term in Eq. 1 is observed for high numerical apertures, for which phase variance may be large. Of course when reducing the aperture one eventually becomes again limited by diffraction (below a characteristic diameter d depending both on aberration level and structure). In this regime, the phase variance on the reduced pupil is small.

As shown in dashed line in Fig. 5, the maximum return flux expectable (i.e. for a very high NA) is higher for lower aberrations, simply denoting the fact that two-photon efficiency is better with a sharper PSF. This observation is also consistent with the selection of a return flux metric by Débarre *et al.*. We show in Fig. 6 the

shape of the image quality criterion, function of the aberration coefficients, that is minimized in the sensorless method. It of course becomes more complex for strong aberrations, which can occur for instance when increasing the numerical aperture in a given sample.

We can then identify three regimes:

- a small phase regime, or conversely a low NA regime, where the waist is limited by diffraction effects. In this regime, the residual phase variance is much lower than $1rad^2$, and a second order Taylor expansion around 0 on the aberration mode coefficients is valid. The optimization metrics used in sensorless approach will then be well approximated by a quadratic form in the coefficients, hence easy to optimize;
- an intermediate regime, with a residual phase variance around $1rad^2$, and where a sensorless approach will still converge provided that the optimization algorithm is robust enough to accommodate the fact that the metric is no longer quadratic (in this regime, for instance, Facomprez *et al.* recommend a 5N algorithm[8]).
- a strong aberration regime, with a residual phase variance much higher than $1rad^2$, and where the waist is limited by aberration effects. The metric for modal sensorless approach is then highly multi-modal, and its optimization with a fast (thus local descent) algorithm is likely to lead to a local extremum and hence to a suboptimal solution. In this regime, the return flux is independent of the aperture size which is favorable for the pupil segmentation approach. Besides the latter method is particularly interesting in this case since it can measure strong aberrations.

These observations suggest that sensorless and pupil segmentation approaches are complementary, and the choice of the technique will depend on the aberration regime, and of course of signal to noise considerations. We discuss in more details their respective application domains in the next paragraph.

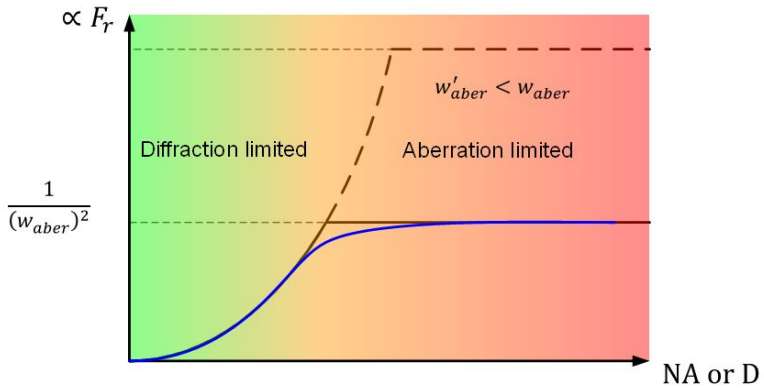

Figure 5. Evolution of the return flux with the numerical aperture for two possible values of w_{aber}.

4. QUALITATIVE COMPARISON

The following paragraph is an attempt to spot strengths and weaknesses of the modal sensorless and the pupil segmentation wavefront sensing approaches. It only concerns the wavefront sensing procedure, of course to be followed by a full aperture AO corrected scientific acquisition sequence.

Return flux As previously mentioned, the return flux assessment is in favor of the modal sensorless approach, although in presence of aberrations the aperture diameter D can be reduced without loss down to a value $d < D$. If the pupil segmentation method is applied with subapertures with a dimension close to d, both methods should benefit from the same return flux;

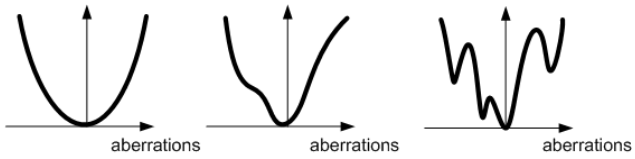

$\mathrm{var}(\varphi) \ll 1\mathrm{rad}^2 \quad \mathrm{var}(\varphi) \cong 1\mathrm{rad}^2 \quad \mathrm{var}(\varphi) \gg 1\mathrm{rad}^2$

Figure 6. Structure of the image quality metric, function of the aberration coefficients, in the three aberration regimes (small, intermediate, strong).

Simplicity, robustness In our view, this point is in favor of the pupil segmentation method, which leads to an explicit wavefront measurement, whereas the modal sensorless approach requires a sequential optimization, which may be all the more complex as the level of aberration is strong;

Hardware complexity The pupil segmentation approach requires a programmable pupil mask, whereas the modal sensorless approach only exploits elements already present in the system (the DM and the imaging system). However, in some cases, the pupil segmentation may be applied with the DM itself, for example with a segmented mirror (by applying a strong tilt to all the segments outside the desired pupil zone);

Field aberration sensing capability In analogy with a Shack-Hartmann wavefront sensor, it is possible to compute field dependent aberrations with the pupil segmentation method by dividing the images in sub-regions, and by estimating the displacement between two images (corresponding to two subapertures) for each sub-region. Optimizing field dependent aberrations is also possible for the modal sensorless approach, for which the quality metric can be computed separately on each sub-region.[7] However, optimization schemes requiring a correction of the current mode at each step make the sensorless method very time consuming for the analysis of field dependent aberrations;

Aliasing The number of modes estimated by the pupil segmentation approach is related to the number of subapertures. This is a major weakness, compared to the modal sensorless approach where any mode achievable by the deformable mirror can be optimized. Additionally, as the pupil segmentation samples the pupil with a limited frequency, higher frequency modes are aliased and may affect low order estimation. This is not the case for the pragmatic modal sensorless approach, which does not rely on a measurement-reconstruction-correction pattern, but directly optimizes an image quality metric;

Sensitivity to the scene contrast This point also is in favor of the modal sensorless approach, where no contrast of the scene is needed if using the return flux as a metric (this is of course no more true when using an image sharpness metric). The pupil segmentation method on the other side requires contrasted features to estimate shifts between sub-pupil images.

To summarize this comparison, the modal sensorless approach should be used in the case for which it has been designed : reasonable aberrations. For stronger aberrations, pupil segmentation method can be used with no return flux loss (with an appropriate setting of the subaperture size). One could of course think of making a joint use of the two techniques, either sequentially starting with pupil segmentation to handle the initial uncorrected strong aberrations, or in more complex hybrid forms where modal sensorless could be used on sub-pupil scans when full aperture aberrations are too strong. Such an hybrid solution is somehow an analog of a recently proposed method, called LIFTed Shack-Hartmann, that combines phase retrieval and Shack-Hartmann wavefront sensing.[10–12]

Of course an important question, beyond the scope of the present paper, is to evaluate the expectable wavefront sensing precision for our biological application: a complex question that depends on the technique and on the aberration amplitude as well as structure, on the flux available, but also on the background noise and on the scene structure.

5. CONCLUSION

We have presented a formal analysis of the two current major wavefront sensing strategies for adaptive optics applied to two-photon scanning microscopy, namely the modal sensorless and the pupil segmentation methods. Based on the one hand on a simple model of the dependence of the return flux with respect to numerical aperture and aberration level, and on the other hand on a qualitative analysis of the shape of image quality metrics as a function of aberration coefficients in various aberration regimes, we have shown that the methods have complementary application domains. Modal sensorless is efficient in the small aberration regime, while pupil segmentation is quite attractive for strong aberrations. We discuss other respective advantages and limitations. Modal sensorless should be less sensitive to aliasing, which is a clear advantage in the presence of high orders, induced for instance by strong index contrasts that often arise in biological tissues. Pupil segmentation should be more favorable to measure field dependent aberrations, of course one has however also to develop means of correcting field dependent aberration during fast scans required to record science movies. The accuracy of wavefront sensing with pupil segmentation depends on the scene structure and flux available, and has yet to be analyzed in detail. We also mention that the two methods can be coupled either sequentially or in more complex hybrid modes. Analogies with similar schemes recently developed for astronomical AO are likely to trigger innovative solutions.

In the coming months, we plan to assess these various strategies by means of simulations, with an aberration model based on *ex vivo* brain slices phase measurements performed by Institut Fresnel, as well as on an experimental demonstrator developed by Institut Fresnel in collaboration with INMED and Onera. The most efficient strategy will then be implemented on INMED's two-photon scanning microscope in order to increase the depth of observation in living mouse hippocampus down to the Dentate Gyrus. It will then be used to acquire *in vivo* movies of the network dynamics in the Dentate Gyrus.

ACKNOWLEDGMENTS

The authors are thankful to our collaborators at Institut Fresnel (Hervé Rigneault, Serge Monneret and Sophie Brasselet) for fruitful discussions, and acknowledge partial support from OMICRON project funded by "CNRS Défi interdisciplinaire ; L'instrumentation aux limites, 2013".

REFERENCES

[1] P. Bonifazi, M. Goldin, M. A. Picardo, I. Jorquera, A. Cattani, G. Bianconi, A. Represa, Y. Ben-Ari, and R. Cossart, "GABAergic hub neurons orchestrate synchrony in developing hippocampal networks," *Science* **326**(5958), pp. 1419–1424, 2009.

[2] S. Feldt Muldoon, I. Soltesz, and R. Cossart, "Spatially clustered neuronal assemblies comprise the microstructure of synchrony in chronically epileptic networks," *Proceedings of the National Academy of Sciences* **110**(9), pp. 3567–3572, 2013.

[3] D. Débarre, E. J. Botcherby, T. Watanabe, S. Srinivas, M. J. Booth, and T. Wilson, "Image-based adaptive optics for two-photon microscopy," *Opt. Lett.* **34**, pp. 2495–2497, Aug 2009.

[4] N. Ji, D. E. Milkie, and E. Betzig, "Adaptive optics via pupil segmentation for high-resolution imaging in biological tissues," *Nature Methods* **7**(2), pp. 141–147, 2009.

[5] J. Tang, R. N. Germain, and M. Cui, "Superpenetration optical microscopy by iterative multiphoton adaptive compensation technique," *Proceedings of the National Academy of Sciences* **109**(22), pp. 8434–8439, 2012.

[6] N. Ji, T. R. Sato, and E. Betzig, "Characterization and adaptive optical correction of aberrations during in vivo imaging in the mouse cortex," *Proceedings of the National Academy of Sciences* **109**(1), pp. 22–27, 2012.

[7] J. Zeng, P. Mahou, M.-C. Schanne-Klein, E. Beaurepaire, and D. Débarre, "3D resolved mapping of optical aberrations in thick tissues," *Biomedical optics express* **3**(8), p. 1898, 2012.

[8] A. Facomprez, E. Beaurepaire, and D. Débarre, "Accuracy of correction in modal sensorless adaptive optics," *Opt. Express* **20**, pp. 2598–2612, Jan 2012.

[9] M. J. Booth, D. Débarre, and A. Jesacher, "Adaptive optics for biomedical microscopy," *Optics and Photonics News* **23**(1), p. 22, 2012.

[10] S. Meimon, T. Fusco, and L. M. Mugnier, "LIFT: a focal-plane wavefront sensor for real-time low-order sensing on faint sources," *Opt. Lett.* **35**(18), pp. 3036–3038, 2010.

[11] C. Plantet, S. Meimon, J.-M. Conan, and T. Fusco, "Experimental validation of LIFT for estimation of low-order modes in low-flux wavefront sensing," *Opt. Express* **21**, pp. 16337–16352, July 2013.

[12] S. Meimon, T. Fusco, V. Michau, and C. Plantet, "Sensing more modes with less sub-apertures : the LIFTed shack-hartmann wavefront sensor," *Opt. Lett.* , 2014. Submitted.